Structure of ^{46}Ti at low excitation energy

N. H. Medina,[1] J. R. B. Oliveira,[1] F. Brandolini,[2] R. V. Ribas,[1] F. Della Vedova,[3] E. Farnea,[2] A. Gadea,[3] S. M. Lenzi,[2] N. Marginean,[4] T. Martinez,[3] D. R. Napoli,[3] M. Nespolo,[3] P. Pavan,[2] and C. A. Ur[2]

[1]*Instituto de Física, Universidade de São Paulo, São Paulo, Brazil*

[2]*Dipartimento di Fisica and INFN, Padova, Italy*

[3]*INFN, Laboratori Nazionali di Legnaro, Legnaro, Italy*

[4]*National Institute for Physics and Nuclear Engineering, Bucharest, Romania*

(Received 25 November 2010; revised manuscript received 16 June 2011; published 19 August 2011)

The nucleus ^{46}Ti has been studied with the reaction ^{42}Ca(^{7}Li,$p2n$)^{46}Ti at a bombarding energy of 31 MeV. Thin target foils backed with a thick Au layer were used. Five new levels of negative parity were observed. Several lifetimes have been determined with the Doppler shift attenuation method. Low-lying experimental negative-parity levels are assigned to three bands with $K^{\pi} = 3^{-}$, 0^{-}, and 4^{-}, which are interpreted in terms of the large-scale shell model, considering particle-hole excitations from $d_{3/2}$ and $s_{1/2}$ orbitals. Shell model calculations were performed using a few effective interactions. However, good agreement was not achieved in the description of either negative- or positive-parity low-lying levels.

DOI: 10.1103/PhysRevC.84.024315 PACS number(s): 21.10.Tg, 21.60.Cs, 23.20.Lv, 27.40.+z

I. INTRODUCTION

The motivation for the present experiment is the spectroscopy of non-yrast levels (a step toward a complete spectroscopy) in order to test cross-shell excitations in the shell model. A good general description of nuclear structure of low-lying levels of *sd* (harmonic oscillator major shell $N = 2$ nuclei (for a review, see Ref. [1]) can be achieved with the universal *sd* (USD) interaction [2]. The *sd* configuration space (CS) is too limited to reproduce high spin states, but a truncated extension to $N = 3(pf$ CS) was recently successful even for reproducing superdeformed bands in ^{36}Ar and ^{38}Ar [3,4]. A further important point is that the doubly magic nucleus ^{40}Ca is known to be constructed by about one third 2-hole 4-hole excitations in the *sd* CS [5] so that the description in a mixed $N = 2$ and $N = 3$ CS (*sdpf* CS) becomes necessary also for low-lying levels of light $1f_{7/2}$ nuclei [6]. Attempts to describe such nuclei achieved only limited success for levels of both parities. A main problem when considering the full *sdpf* CS is that the matrix dimensions are too large, so that selected configurations have to be chosen. The status of the shell model (SM) description in this nuclear region was well reviewed in Ref. [7]. In contrast, great success was obtained for natural parity levels in the middle and the second half of the $1f_{7/2}$ orbital in the *pf* CS up to the termination in the $1f_{7/2}^{n}$ CS [8]. The observed level schemes agree well with the predictions of the large-scale shell model (LSSM) [9,10]. Good success was also obtained in the description of unnatural parity levels, taking into account a single-hole excitation in the *sd* CS. The level schemes of these nuclei are thus little influenced by other orbitals.

The $1f_{7/2}$ nuclei have been widely explored using fusion reactions induced by heavy ions. Several new and interesting results have been achieved at Laboratori Nazionali di Legnaro (LNL) owing to the capability of such reactions to populate high spin states and yrast levels [11–18]. On the other hand, theoretical calculations predict, at low energy, some structures that cannot be efficiently populated in heavy ion reactions. As light projectiles lead to the population of low-lying levels, we have studied ^{49}Cr also with the α, n reaction leading to the observation of nearly all levels up to 4 MeV [19].

The focus of the present investigation is to measure the low-lying levels in ^{46}Ti populated with a light projectile, analogous to the quoted study of ^{49}Cr [19]. As discussed in Ref. [18], the yrast $K^{\pi} = 3^{-}$ band of the ^{46}Ti nucleus can be described as due to a proton promotion from the [2 0 2]$3/2^{+}$ Nilsson orbital to the [3 2 1]$3/2^{-}$ orbital, followed by parallel coupling of the angular momenta. Some yrare negative-parity levels were previously reported, which were not appreciably populated in the quoted measurements and whose spin assignments are contradictory [20]. According to SM calculations [18], a $K^{\pi} = 0^{-}$ band is also expected at low excitation energy, originating from the same mechanism as the $K^{\pi} = 3^{-}$ band, but with an antiparallel coupling, as well as a $K^{\pi} = 4^{-}$ band.

II. EXPERIMENTAL PROCEDURE

The non-yrast states of ^{46}Ti were populated with the ^{42}Ca(^{7}Li,$p2n$) reaction at 31-MeV beam energy. The beam was provided by the LNL 15 MV XTU-Tandem, with a current of about 2p nA on target. The target consisted of a 0.8 mg/cm^2 layer of 95% enriched ^{42}Ca on a 3.5 mg/cm^2 backing of Au.

The γ rays were detected with the GASP (gamma-ray spectrometer) array, comprising 40 Compton-suppressed hyper-pure germanium (HPGe) detectors and an 80-element bismuth germanium oxide (BGO) ball, which acts as a γ-ray multiplicity filter. Events were stored on tape when at least two Ge detectors and two elements of the multiplicity filter fired simultaneously.

In order to allow lifetime analysis, data were sorted into seven γ-γ matrices, having on the first axis detectors in rings at 34°, 60°, 72°, 90°, 108°, 120°, and 146° and on the second axis any of the other 39 detectors.

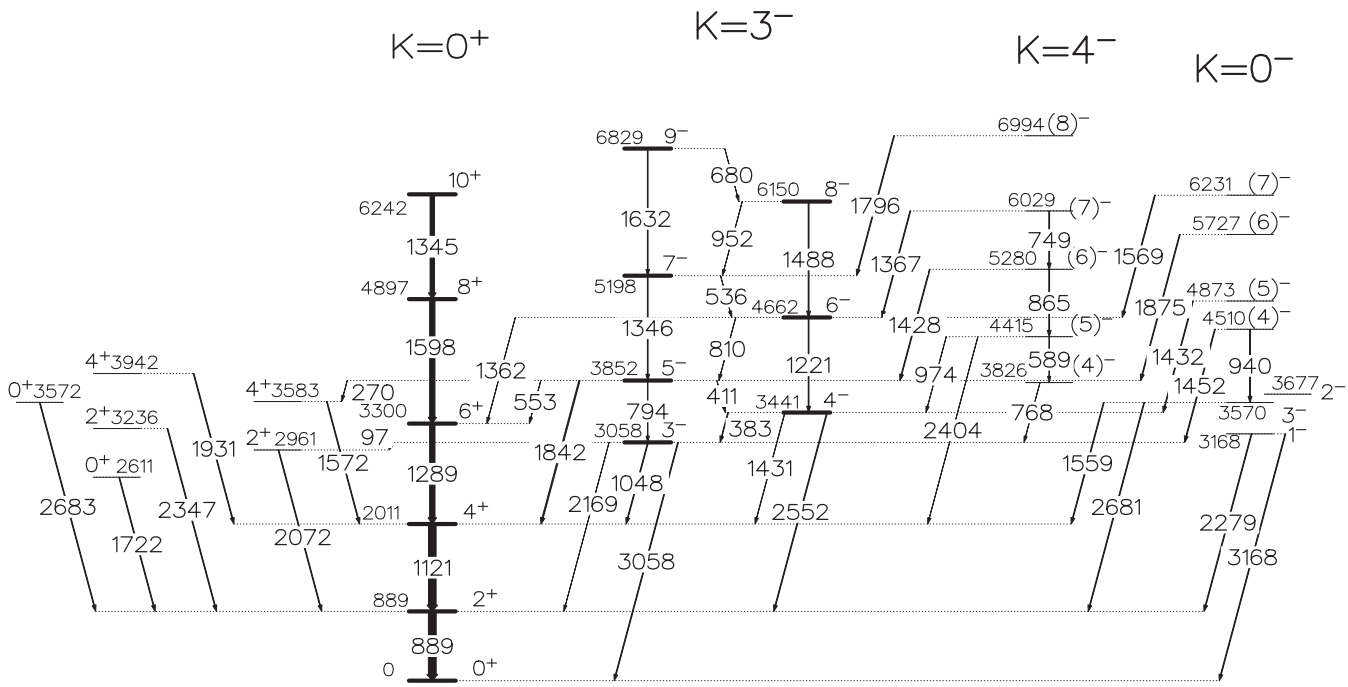

FIG. 1. Partial level scheme of ^{46}Ti at low excitation energy.

III. EXPERIMENTAL RESULTS

A. The ^{46}Ti level scheme

Figure 1 presents the partial-level scheme of ^{46}Ti, mostly extracted from Refs. [17] and [18]. Only levels up to about 7.0 MeV of excitation energy are shown, to emphasize the results of the present work with regard to the two nearby bands with $K^\pi = 0^-$ and $K^\pi = 4^-$. States up to $I = 14$ ($E^* = 12$ MeV) were observed in the present measurement. The $K^\pi = 0^+$ ground-state (gs) band and the $K^\pi = 3^-$ band were already investigated in detail in Ref. [18]. The predicted 0^- level has not been observed. The transitions reported in Ref. [20], depopulating the 7^- and 8^- states, were not confirmed. The 2^- and 1^- levels and the 2279- and 3168-keV transitions, not observed in this experiment, were taken from Ref. [21]. All the other transitions presented in Fig. 1 were observed in the present experiment. New levels were found at 4510, 4873, 5727, 6231, and 6994 keV and are tentatively assigned to spins (4), (5), (6), (7), and (8), respectively, all with negative parity, on the basis of the arguments discussed later. An additional transition of $E_\gamma = 270$ keV was observed connecting the 5^- level at 3852 keV to the level at 3583 keV.

B. Doppler Shift Attenuation Method (DSAM) lifetime measurements in ^{46}Ti

The LINESHAPE program [22] was used for Doppler Shift Attenuation Method lifetime measurement analysis. The Northcliffe-Schilling stopping power [23], corrected for atomic shell effects, was used [24]. Figures 2, 3, and 4 present examples of line-shape fits, corresponding to the $4_2^- \rightarrow 3_1^-$, $5_2^- \rightarrow 4_1^-$, and $5_3^- \rightarrow 4_1^-$ transitions, respectively, observed at forward and backward angles.

In Table I, all of the information obtained on the lifetimes of the $K^\pi = 0^-$ and $K^\pi = 4^-$ bands are reported. The $B(M1)$ reduced transition probabilities were calculated from the observed lifetimes ($\tau_{\rm exp}$) and branching ratios (BR), assuming no admixture of $E2$ multipolarity ($\delta = 0$).

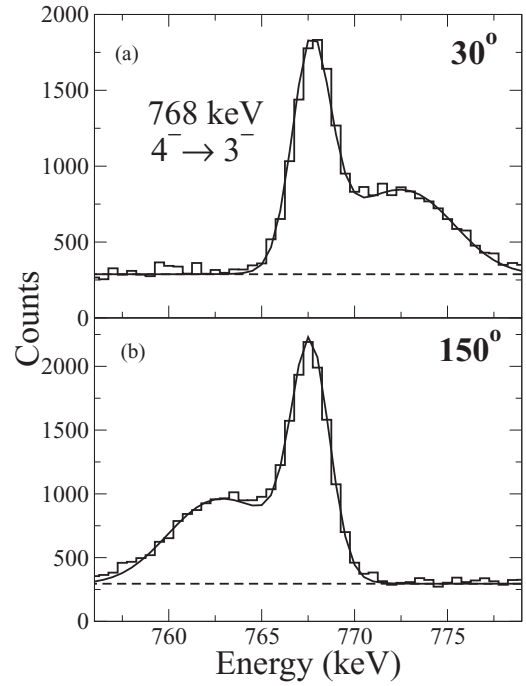

FIG. 2. Standard DSAM line-shape fits for the 768-keV $4_2^- \rightarrow 3_1^-$ transition in ^{46}Ti observed at (a) 30° and (b) 150°.

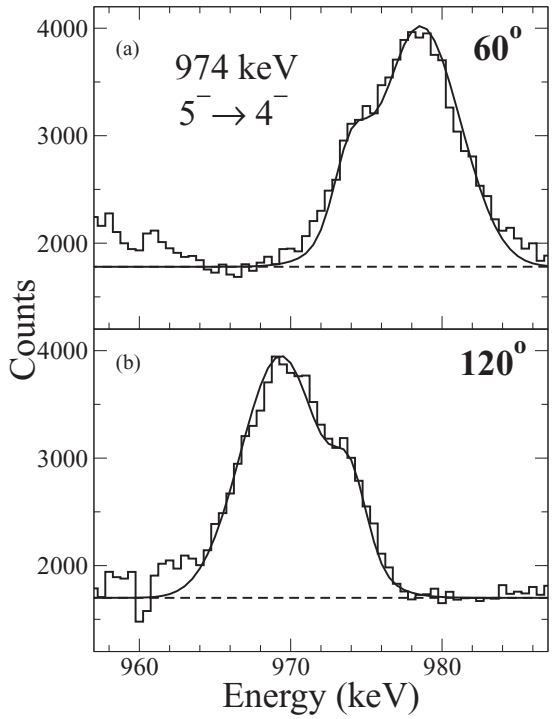

FIG. 3. Standard DSAM line-shape fits for the 974-keV $5_2^- \rightarrow 4_1^-$ transition in ^{46}Ti observed at (a) 60° and (b) 120°.

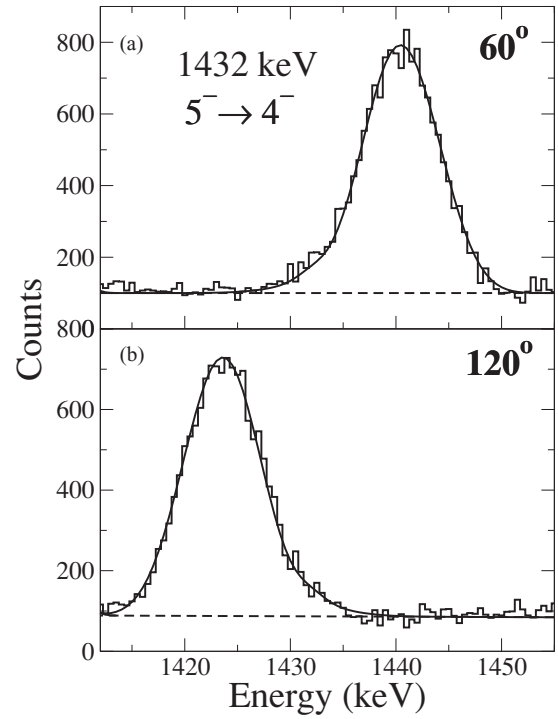

FIG. 4. Standard DSAM line-shape analysis for the 1432-keV $5_3^- \rightarrow 4_1^-$ transition in ^{46}Ti observed at (a) 60° and (b) 120°.

Table II summarizes the available information on the non-yrast positive-parity levels. The theoretical values are discussed in the next section.

C. New levels in ^{46}Ti

Level parities are assigned on the basis of an assumed upper limit (UL) for E1 strengths of 3×10^{-4} W.u. The yrare levels 4_2^-, 5_2^-, 6_2^-, and 7_2^-, at 3826, 4415, 5280, and 6029 keV, respectively, were proposed long ago to belong to a rotational sequence [25].

The level at 3583 keV is assigned to be 4^+. Since the lifetime of this level is reported to be very short [70(30) fs], the 2683-keV [21] and 1572-keV transitions from that state to the 2^+ and 4^+ gs band states, respectively, have to be of $E2$ or $M1$ multipolarity. The $M2$ multipolarity for the 270-keV transition can be excluded because it would be extremely weak—well below our observational limit. Therefore, overall consistency is possible only with $I^\pi = 4^+$ for the 3583-keV state. No new levels of positive parity were observed.

According to Ref. [18], the new levels have to be assigned to a $K = 4^-$ or to a $K = 0^-$ band, but the interpretation is not so straightforward in view of our present calculations. The experimental yrare $(4)^-$ state is assigned to a $K = 4^-$ band head (due to the pattern of observed $M1$ in-band transition links) while the third $(4)^-$ excitation at 4510 keV is assigned to a $K = 0^-$ band, whose band head was not observed. $K = 4^-$ bands can be produced by exciting either a neutron or a proton from the Nilsson $[2\,0\,2]3/2^+$ orbital to the empty $[3\,1\,2]5/2^-$ orbital. A signature of the $K = 4^-$ band head is its large positive spectroscopic quadrupole moment Q. The antiparallel coupling gives rise to $K = 1^-$ bands, whose lowest state, 1^-, was predicted at about 1 MeV above the $K = 4^-$ band head, but not observed.

IV. DISCUSSION

A. Shell model calculations

Several interactions have been used in this mass region, nearly all of them with some specific adaptations [7,26–33]. The multitude of interactions and the proliferation of their variations means that the theoretical description, after nearly 50 years of SM calculations, is still under development in this nuclear region. Many such interactions have been recently reviewed [10,34]. Several of them are available in the ANTOINE code [35] web site [36].

Here we present the calculations performed with ANTOINE and the SDPF-SM interaction, which was used to describe deformed bands in ^{36}Ar [37]. The parameters of this interaction were kindly provided by the authors [38]. In this case, the $d_{5/2}$ orbital was closed, making ^{28}Si the inert core. This interaction was proposed, as were several others, by the Strasbourg-Madrid group, and originated from the interaction of Ref. [26], which mainly consists of the USD and KB3 [39] interactions for intra-shell two-body matrix elements (TBME) in the sd and pf configuration spaces, respectively, together with the Kahana, Lee and Scott interaction for the cross shell TBME [27]. In addition, binding energies and some cross-monopoles were modified in order to reproduce levels in ^{41}Ca. Free g factors and effective charges of $q_{\rm eff}^\pi = 1.5$ and $q_{\rm eff}^\nu = 0.5$ were adopted. Another interaction, named SDPF-NR [28], was also used with similar results.

TABLE I. Reduced magnetic transition probabilities for ^{46}Ti. A mixing ratio of $\delta^2 = 0$ was assumed to evaluate the experimental values. Previous lifetime values were extracted from Ref. [21]. The theoretical values are presented for a single hole in the $d_{3/2}$ (Th. 1) or $s_{1/2}d_{3/2}$ (Th. 2) configuration space with the SDPF-SM interaction, both for the $B(M1)$ and $B(E2)$, together with the corresponding theoretical mixing ratio $\delta^2 = I(E2)/I(M1)$ (taking into consideration the experimental transition energy).

State	E_{level}	τ_{exp}	τ_{exp} prev.		E_γ	BR	B(M1) Exp.	B(M1) Th. 1	B(E2)		B(M1) Th. 2	B(E2)	
I_n^π	(keV)	(*ps*)	(*ps*)	Transition	(keV)	(%)	(μ_N^2)	(μ_N^2)	(e^{2}fm^4)	δ^2	(μ_N^2)	(e^{2}fm^4)	δ^2
$K^\pi = 4^-$													
4_2^-	3826	1.49(8)	3.7(21)	$4_2^- \to 3_1^-$	768	100	0.083(4)	0.001	12.7	1.03	0.001	20.3	1.7
5_2^-	4415	0.50(5)	0.45(17)	$5_2^- \to 4_1^-$	974	60.5(21)	0.074(8)	0.014	19.3	0.09	0.023	28.5	0.08
				$5_2^- \to 4_2^-$	589	33.0(18)	0.182(20)	0.52	0.23	0.00	0.3	1.28	0.00
6_2^-	5280	0.31(5)		$6_2^- \to 5_1^-$	1428	87.3(23)	0.054(11)	0.023	25.3	0.15	0.037	49.3	0.19
				$6_2^- \to 5_2^-$	865	12.7(43)	<0.056	0.57	3.7	0.00	0.43	4.1	0.00
7_2^-	6029	0.18(2)		$7_2^- \to 6_1^-$	1367	91.9(3)	0.112(12)	0.024	19.8	0.11	0.037	23.8	0.08
				$7_2^- \to 6_2^-$	749	8.1(9)	0.060(9)	0.41	0.61	0.00	0.21	0.69	0.00
8_2^-	6994	0.23(3)		$8_2^- \to 7_1^-$	1796	100	0.042(6)	0.043	30.3	0.16	0.054	54.8	0.23
$K^\pi = 0^-$													
1_1^-	3168		0.176(24)	$1_1^- \to 2_1^+$	2279	100(2)							
				$1_1^- \to 0_1^+$	3168	83(2)							
3_2^-	3570		50^{+19}_{-16}	$3_1^- \to 4_1^+$	1559	100							
				$3_1^- \to 2_1^+$	2681	27							
4_3^-	4510	0.31(3)		$4_3^- \to 3_1^-$	1452	55.7(1)	0.033(3)	0.33	0.02	0.000	0.000	3.8	>1.3
				$4_3^- \to 3_2^-$	940	44.3(19)	0.097(10)	0.001	0.0025	0.000	0.019	30.3	0.1
5_3^-	4873	0.22(2)		$5_3^- \to 4_1^-$	1432	100	0.087(8)	0.25	1.18	0.001	0.062	1.61	0.004
6_3^-	5727	<0.15		$6_3^- \to 5_1^-$	1875	100	>0.057	0.000	0.017	>0.01	0.040	4.66	0.028
7_3^-	6227	0.31(3)		$7_3^- \to 6_1^-$	1569	100	0.047(5)	0.20	1.27	0.001	0.010	0.13	0.002

B. Positive-parity levels

In an even-even nucleus such as ^{46}Ti, the first task of SM calculations is to reproduce the properties of the ground-state band and low-lying states of positive parity. It was suggested in Ref. [8] that the yrast 2^+ and 4^+, as well as the yrare 0^+ states, have ^{40}Ca core-mixing components. This is a phenomenon similar, even if less pronounced, to the one discussed in Ref. [40,41] on ^{42}Ca. However, such a mixing is difficult to evaluate quantitatively. In the SM approach, those states should be described at least in the two full major shells *sd* and *pf*, but such calculations are difficult for ^{46}Ti. The dimension of the matrices in the full two major shells in the *M* scheme is larger than 10^{12}, such that severe truncations have to be applied. Moreover, a satisfactory effective interaction that could adequately account for the applied truncations is not yet available.

The shell model calculations were performed in a limited configuration space consisting of $d_{3/2}$ and $f_{7/2}$ orbitals but, on the other hand, full *sdpf* calculations are not possible. Figure 5 compares the experimental and theoretical level schemes for the non-yrast states of positive parity. The calculations were performed with the SDPF-SM residual interaction. The transition probabilities are presented in Table II. The overall agreement is very poor. Very similar results were also obtained with the SDPF-NR interaction.

C. Negative-parity levels

The calculations for negative-parity levels of ^{46}Ti require simultaneous consideration of the two major shells *sd* and *pf*. A first approximation was made by extending the full

TABLE II. Reduced electric transition probabilities in ^{46}Ti.

I^π	E (level) (keV)	τ(fs)	Transition	E_γ (keV)	BR (%)	$B(E2)$ (e^{2}fm^4)	$B(E2)$ Th. 1
0_3^+	3572	192^{+16}_{-13}	$0_3^+ \to 2_1^+$	2683	100	30.7(23)	0.092
0_2^+	2611	76(21)	$0_2^+ \to 2_1^+$	1722	100	710(200)	9.6
2_3^+	3236	29(6)	$2_3^+ \to 0_1^+$	3236	18.8(13)	12.6(28)	6.4
			$2_3^+ \to 2_1^+$	2347	100.0(13)	<300	19.4
4_3^+	3942	<20	$4_3^+ \to 4_1^+$	1931	100		
2_2^+	2961	166(7)	$2_2^+ \to 0_1^+$	2961	4.4(6)	0.91(13)	5.3
			$2_2^+ \to 2_1^+$	2072	100.0(6) ($\delta = -1.21(14)$)	73.4(31)	63.1
4_2^+	3584	70(30)	$4_2^+ \to 4_1^+$	1572	100	<1200	28.7

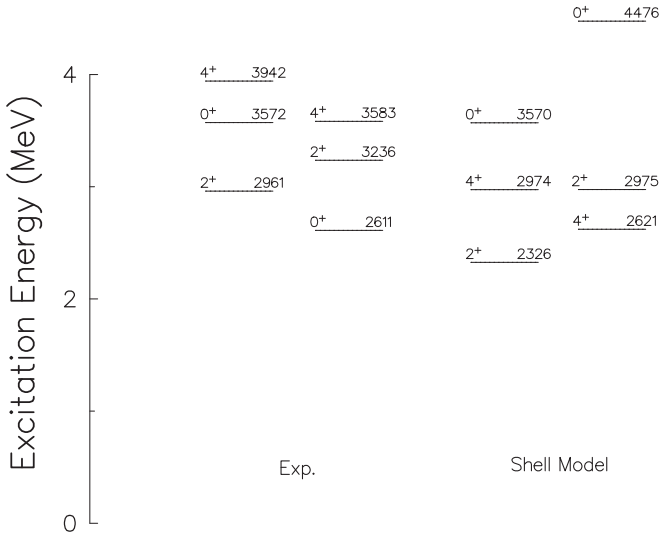

FIG. 5. Comparison of experimental and theoretical non-yrast positive-parity states. The calculations were performed in the $s_{1/2}$, $d_{3/2}$, $f_{7/2}$, and $p_{3/2}$ space with the SDPF-SM residual interaction.

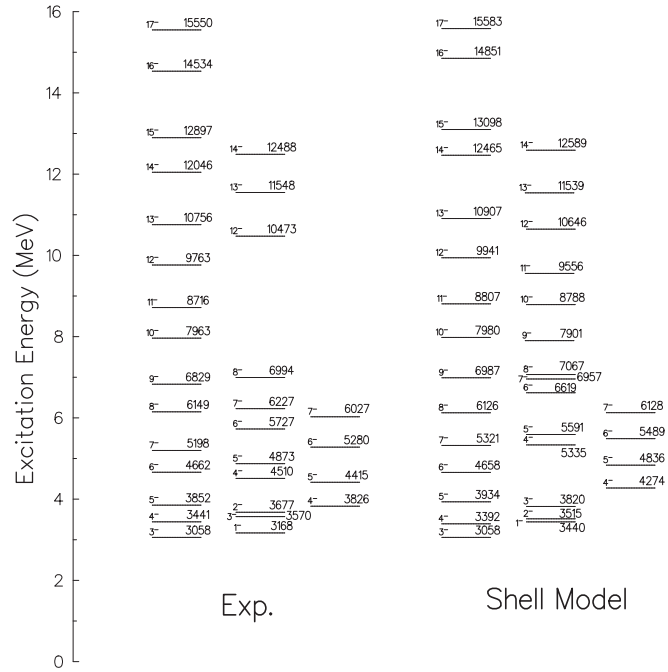

FIG. 6. Comparison of experimental and theoretical negative-parity bands. The levels 9^-_2, 10^-_2, and 11^-_2 were predicted but not observed. Only the result of the simplest calculational approach (one $d_{3/2}$ hole, coupled to the full *pf* shell) is presented, with the SDPF-SM interaction (a very similar scheme is obtained with the SDPF-NR interaction).

pf configuration space with the inclusion of a single hole in the $d_{3/2}$ orbital. This is essentially the same approach used in Ref. [18] (with only minor modifications of the interaction), and the results are, of course, similar. With this truncation, a rather satisfactory agreement for low-lying unnatural parity structures was previously obtained in several nuclei, for example, the odd nuclei ^{47}V, ^{49}Cr, and ^{51}Mn, where the lowest bands are described by coupling the $K^\pi = \frac{3}{2}^+$ hole to the corresponding Nilsson orbital. Experimental and theoretical level schemes for negative-parity states in ^{46}Ti are compared in Fig. 6. The agreement is reasonable. The experimental $B(M1)$ values, however, are not well reproduced (Th. 1 in Table I). The calculations show little sensitivity when using effective g factors for protons or neutrons. The theoretical $B(E2)$, together with the theoretical mixing ratio $I(E2)/I(M1) = \delta^2$, that is, the ratio of the intensities of the two multipolarities (considering the experimental transition energies), is also presented in the table. Some of the predicted $E2$ intensities are larger than the corresponding $M1$ ones, for example, for the $4^-_2 \rightarrow 3^-_1$ transition (where they are comparable). However, even considering such admixtures, the agreement with the observed lifetimes is poor. The calculated static quadrupole moment Q for the third $I^\pi = 4^-$ state is large (47 e^2 fm^4) and, therefore, consistent with a $K^\pi = 4^-$ band-head assignment.

It has been shown, however, that in ^{45}Ti and ^{49}Cr it is necessary to include the $2s_{1/2}$ orbital to reproduce the experimental low-lying $K^\pi = \frac{1}{2}^+$ band [8]. In those calculations, the effective interaction of Ref. [42] was used where, in some cases, an adjustment was performed in a few monopole terms to better describe the sideband energies. The matrix elements in the *pf* shell are essentially those from the KB3G interaction, proposed by the Strasbourg-Madrid group [43], while those connecting to the nucleon hole are taken from Ref. [27]. Therefore, a second, less severe space truncation was considered for ^{46}Ti with the inclusion of the $2s_{1/2}$ orbital. However, no change in the SDPF-SM or SDPF-NR interactions was attempted. No large positive spectroscopic quadrupole moment was found among the lowest four states with $I^\pi = 4^-$, pointing to a strong configuration mixing. The previous assignment of a large-Q, $K^\pi = 4^-$ band is thus not corroborated by this result. The level energies and $B(M1)$ values obtained in this second space truncation are similar to those of the first one [Th. 2 in Table I].

V. CONCLUSIONS

The spectroscopy of ^{46}Ti, lying in the middle of the $1f_{7/2}$ shell, has been extended using light particle-induced reactions, particularly through the determination of electromagnetic transition rates. At low excitation energy, the LSSM predicts many negative-parity levels, which can be tentatively organized in bands. With the present status of computational capabilities and of knowledge of the residual interaction for light $1f_{7/2}$ nuclei, it is very difficult to find an approach that provides a good description of all aspects of the experimental results simultaneously, such as level scheme of yrast and non-yrast state energies, transition probabilities, and spectroscopic quadrupole moments. In this context, the success of SM truncated to the *pf* CS for nuclei in the second half of the $1f_{7/2}$ shell appears to be even more spectacular.

ACKNOWLEDGMENTS

J.R.B.O., N.H.M., and R.V.R. acknowledge financial support from Istituto Nazionali di Fisica Nucleare (INFN), Italy, and from the Brazilian agencies Conselho Nacional de Desenvolvimento Científico e Tecnológico (CNPq) and Fundação de Amparo à Pesquisa no Estado de São Paulo (FAPESP). The authors thank Frederic Nowacki for fruitful discussions.

[1] B. A. Brown and B. H. Wildenthal, Annu. Rev. Nucl. Part. Sci. **38**, 29 (1988).
[2] B. H. Wildenthal, Prog. Part. Nucl. Phys. **11**, 5 (1984).
[3] C. E. Svensson *et al.*, Phys. Rev. C **63**, 061301 (2001).
[4] D. Rudolph *et al.*, Phys. Rev. C **65**, 034305 (2002).
[5] W. J. Gerace and A. M. Green, Nucl. Phys. A **93**, 110 (1967).
[6] E. Caurier, J. Menendez, F. Nowacki, and A. Poves, Phys. Rev. C **75**, 054317 (2007).
[7] B. A. Brown, Prog. Part. Nucl. Phys. **47**, 517 (2001).
[8] F. Brandolini and C. A. Ur, Phys. Rev. C **71**, 054316 (2005).
[9] E. Caurier *et al.*, Phys. Rev. Lett. **75**, 2466 (1995).
[10] E. Caurier, G. Martínez-Pinedo, F. Nowacki, A. Poves, and A. P. Zuker, Rev. Mod. Phys. **77**, 427 (2005).
[11] F. Brandolini *et al.*, Nucl. Phys. A **642**, 387 (1998).
[12] F. Brandolini *et al.*, Phys. Rev. C **60**, 041305(R) (1999).
[13] F. Brandolini *et al.*, Nucl. Phys. A **693**, 571 (2001).
[14] F. Brandolini *et al.*, Phys. Rev. C **64**, 044307 (2001).
[15] F. Brandolini *et al.*, Phys. Rev. C **66**, 024304 (2002).
[16] F. Brandolini *et al.*, Phys. Rev. C **66**, 021302 (2002).
[17] D. Bucurescu *et al.*, Phys. Rev. C **67**, 034306 (2003).
[18] F. Brandolini *et al.*, Phys. Rev. C **70**, 034302 (2004).
[19] F. Brandolini *et al.*, Phys. Rev. C **73**, 024313 (2006).
[20] J. A. Cameron *et al.*, Phys. Rev. C **44**, 1882 (1991).
[21] S.-C. Wu, Nucl. Data Sheets **91**, 1 (2000).
[22] J. C. Wells and N. Johnson, Report No. ORNL-6689, 44 (1991).
[23] L. C. Northcliffe and R. F. Schilling, Nucl. Data Tables A **7**, 233 (1970).
[24] S. H. Sie *et al.*, Nucl. Phys. A **291**, 11 (1977).
[25] G. D. Dracoulis, D. C. Radford, and A. R. Poletti, J. Phys. G **4**, 1323 (1978).
[26] J. Retamosa, E. Caurier, F. Nowacki, and A. Poves, Phys. Rev. C **55**, 1266 (1997).
[27] S. Kahana, H. Lee, and C. Scott, Phys. Rev. **185**, 1378 (1969).
[28] S. Nummela *et al.*, Phys. Rev. C **63**, 044316 (2001).
[29] F. Nowacki and A. Poves, Phys. Rev. C **79**, 014310 (2009).
[30] E. Caurier *et al.*, Phys. Lett. B **522**, 240 (2001).
[31] Y. Utsuno, T. Otsuka, T. Mizusaki, and M. Honma, Phys. Rev. C **60**, 054315 (1999).
[32] E. K. Warburton, J. A. Becker, and B. A. Brown, Phys. Rev. C **41**, 1147 (1990).
[33] D. J. Dean *et al.*, Phys. Rev. C **59**, 2474 (1999).
[34] A. Poves, E. Caurier, F. Nowacki, and A. Zuker, Eur. Phys. J. A **20**, 119 (2004).
[35] E. Caurier and F. Nowacki, Acta Phys. Pol. **30**, 705 (1999).
[36] [http://sbgat194.in2p3.fr/~theory/antoine/menu.html].
[37] C. E. Svensson *et al.*, Phys. Rev. Lett. **85**, 2693 (2000).
[38] F. Nowacki (private communication).
[39] A. Poves and A. P. Zuker, Phys. Rep. **70**, 235 (1981); Nucl. Phys. A **694**, 157 (2001).
[40] W. J. Gerace and A. M. Green, Nucl. Phys. A **113**, 641 (1968).
[41] P. Federman and S. Pittel, Phys. Rev. **186**, 1106 (1969).
[42] A. Poves and J. S. Solano, Phys. Rev. C **58**, 179 (1998).
[43] A. Poves, J. Sanchez Solano, E. Caurier, and F. Nowacki, Nucl. Phys. A **694**, 157 (2001).